Some applications of discontinuous Galerkin methods in solid mechanics

Adrian Lew[1], Alex Ten Eyck[1], and Ramsharan Rangarajan[1]

Mechanical Engineering, Stanford University {lewa,alabute,rram}@stanford.edu

1 Introduction

Discontinuous Galerkin methods are finite element methods distinguished by the use of piecewise discontinuous functions across element boundaries to approximate the solution of a boundary value problem. Discontinuous Galerkin methods have been remarkably successful as high-order versions, and natural generalizations to unstructured meshes, of finite volume methods for hyperbolic conservation laws (see [5]). In this case, discontinuities across element boundaries permit the crafting of conservative and monotone schemes by adopting piecewise constant approximations within each element, as well as the simple use of slope limiters to achieve stability for high-order schemes. Hence, the introduction of discontinuous fields across element boundaries provides a clear set of algorithmic advantages.

Similar algorithmic advantages are encountered in the context of elliptic problems with constraints, for example, incompressible elasticity. In this case in addition to the mechanical equilibrium equation, the solution must satisfy the incompressibility constraint. It is well know that if piecewise affine conforming (i.e., continuous) finite elements are adopted, then the subset of the discrete space that satisfies the constraint almost everywhere may become so poor that its approximation properties are severely deteriorated. This is commonly known as locking. One way around this problem is by trading the importance of constraints, namely, it is possible to relax the continuity constraint across element boundaries to strongly impose the incompressibility one without any loss in accuracy (order of convergence), see [20, 11, 9]. This idea of *trading* the enforcement of the inter-element continuity constraint to strongly impose others, without any loss of accuracy, is a pattern that repeatedly appears in many applications for which DG methods display a clear algorithmic advantage.

A second such example is found in the solution of some structural models of shells, plates and beams [8, 14, 18, 2, 4, 10]. The constraint in this case is the compatibility relation between the rotational and displacement degrees

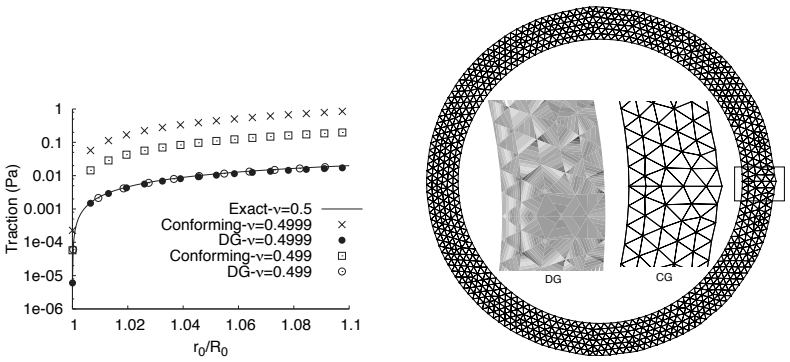

Fig. 1. On the left, evolution of the traction at the inner wall of the cylinder as a function of the relative expansion of the inner radius. Results computed with conforming (CG) and discontinuous (DG) Galerkin methods are shown, for two near incompressible cases, $\nu = 0.499, 0.4999$, where ν is the Poisson ratio. The exact solution is also shown for comparison. It is apparent from these results that the method is locking–free in the finite strain case. The use of discontinuities to enforce the incompressibility constraint is clearly revealed in the figure on the right, which depicts the deformed mesh in the CG case, with enlarged views of the area enclosed by a square for both CG and DG approximations. The small protruding cusp in the CG mesh testifies to the large stresses created within to satisfy the incompressibility constraint. In contrast, these are easily relaxed through discontinuities in the DG case, as the contour plots therein reveal

of freedom, which is nearly exactly enforced as the thickness of the structure becomes very small. Known as shear locking, it can be overcome by again relaxing the continuity constraint along element boundaries and switching to a DG formulation. A third such example arises in the context of immersed boundary methods, as we shall demonstrate later in the manuscript. In this case the constraints are the Dirichlet boundary conditions on the immersed boundary, which may lead to a deteriorated convergence rate. Optimal convergence rates are recovered once a discontinuous Galerkin discretization is introduced. Finally, in the context of high-order equations, such as for gradient plasticity theories [6, 7] and some phase transition models [19], the introduction of discontinuities in the approximation of the derivative helps overcome the difficulties in constructing conforming spaces with continuous derivatives on unstructured meshes.

The goal of this article is to highlight some of the main ideas and showcase some examples of our own work on the subject. With this in mind, section 2 introduces a few highlights of the method, in the form of numerical examples. In section 3, we formally present the class of discontinuous Galerkin methods which have been adopted in this article. Their application for nonlinear elastic problems is described in section 4, where we also briefly discuss the crucial

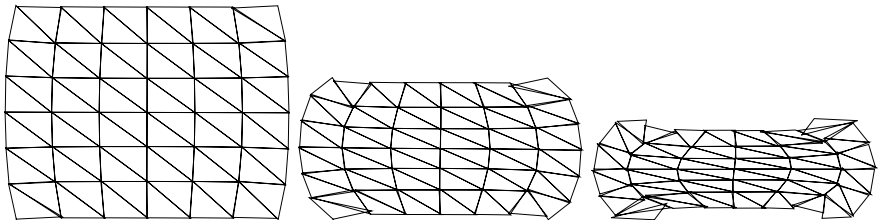

(a) Snapshots for the discontinuous Galerkin solution

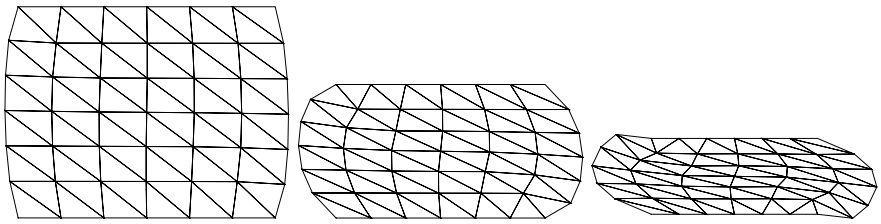

(b) Snapshots for the continuous Galerkin solution

Fig. 2. Compression of an elastic block. Comparison between the continuous and discontinuous Galerkin solutions obtained with affine shape functions within each element

subject of stabilization. Finally, section 5 briefly describes a discontinuous-Galerkin-based immersed boundary method.

2 Examples

Incompressibility constraint at finite strains. The following example from [9] illustrates how discontinuities across element boundaries are actually used to accommodate the nonlinear incompressibility constraint at large deformations. We consider a cylinder under plane strain, made of a nearly incompressible neo-Hookean material, whose external wall is traction free. The internal boundary, in contrast, is deformed to acquire a new radius r_0 from its traction-free value of R_0. Both continuous and discontinuous Galerkin methods with an affine interpolation within each element were adopted. The results are depicted and explained in Fig. 1.

Mesh-based kinematic constraints. The following example from [9] displays an unusual constraint, introduced by the choice of the mesh. An elastic block made of a compressible neo-Hookean material is squeezed by imposing displacements on its top and bottom faces, as shown in Fig. 2. Because of the lack of symmetry of the mesh, the symmetry of the exact problem is lost at some point during the loading path when continuity is enforced, while it is mostly restored when the latter is relaxed.

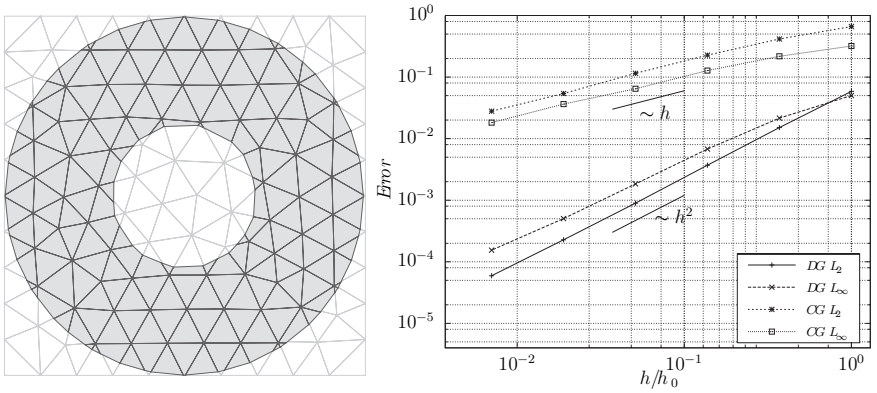

Fig. 3. A simulation with a DG-based immersed boundary method. The domain of the problem, a circular ring, is immersed in an arbitrary mesh, as shown on the left. Made of a linear elastic material, the ring is stretched by imposing Dirichlet boundary conditions on its entire boundary. The L_2 and L_∞ errors in the solutions as a function of the mesh size are shown on the right, for both CG and DG approximation spaces constrained to satisfy the Dirichlet boundary conditions on the approximate boundary of the domain. The CG method displays a sub-optimal convergence rate, again recovered by simply relaxing the continuity constraint across element boundaries. In this case, a DG approximation is only adopted in those elements intersected by the boundary

Boundary conditions as constraints. The term immersed boundary methods broadly describes methods in which the boundary of the domain may cut through elements in the mesh; see Fig. 3. The problem of generating a mesh in a complicated geometry is in this way circumvented. It is replaced, however, by the need to devise strategies to impose boundary conditions on the immersed boundary. The natural idea of simply constraining the continuous finite element space over the mesh to satisfy prescribed Dirichlet boundary generally leads to suboptimal approximation properties, known as boundary locking. This is not the case when a DG discretization is adopted, as clearly showcased in Fig. 3 and described in [12].

Competitive performance. Not every problem presents a set of competing constraints for which it is convenient to relax the continuity across element boundaries. A known drawback of DG methods in these cases is that often they have a significantly larger number of degrees of freedom than CG methods *on the same mesh*. These additional degrees of freedom are generally used to obtain a better approximation of the solution. When CG and DG solutions with the same number of degrees of freedom are compared, the former is generally more accurate, but the latter is often competitive. This is illustrated in Fig. 4 from [17], for a two-dimensional case. The contrast in the performance of both methods is often larger for three-dimensional computations.

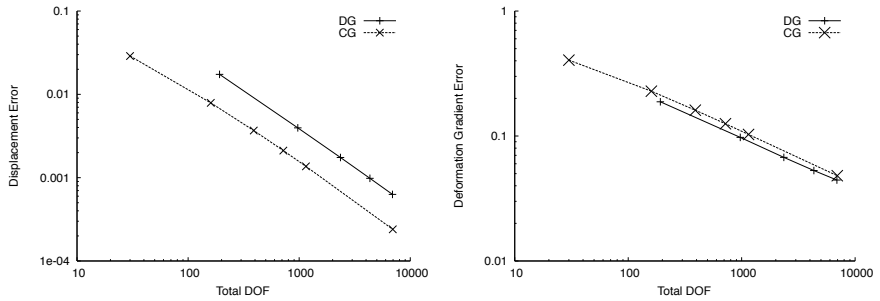

(a) L^2-error in displacements (b) L^2-error in the deformation gradient

Fig. 4. Convergence plot for the displacements (left) and deformation gradient (right) as a function of the number of degrees of freedom for a two-dimensional nonlinear elasticity example. For this case, the CG approximation is more efficient than the DG one for the computation of displacements, while the situation is reversed in the case of the deformation gradient

Large-scale simulations. We show next an application that benefits from the lack of locking for incompressible elastic materials of DG discretizations, and simultaneously demonstrates the possibility of utilizing them for the solution of large solid mechanics problems. It consists of the simulation of the mechanical response of a $50^3\,\mu\text{m}^3$ sample of blood-vessel microstructure (the media), obtained with novel scanning electron microscopy techniques [15]. Regions that contain elastin have been segmented, as shown in black in Fig. 5. This rather heterogeneous microstructure was meshed with 175,616 trilinear hexahedra, totaling 4,214,784 degrees of freedom when the DG discretization was adopted. As a first step towards a more comprehensive study, elastin was assumed to be an isotropic linear elastic material immersed in incompressible water. With proper preconditioning of the linear system [17], the deformation of the sample could be solved in 512 processors in approximately one hour, allowing us to perform multiple simulations in one day.

3 Formulation of discontinuous Galerkin methods

The essential component in the construction of a DG method is the specification of how derivatives of functions are approximated. Since functions in the DG space may be discontinuous across element boundaries, their distributional derivatives may contain a singular part in the form of delta functions. Consequently, instead of approximating the derivative of a smooth function u with the exact distributional derivative of its discrete approximation u_h, we do so with another possibly piecewise discontinuous function, which we denote $D_{\text{DG}}u_h$.

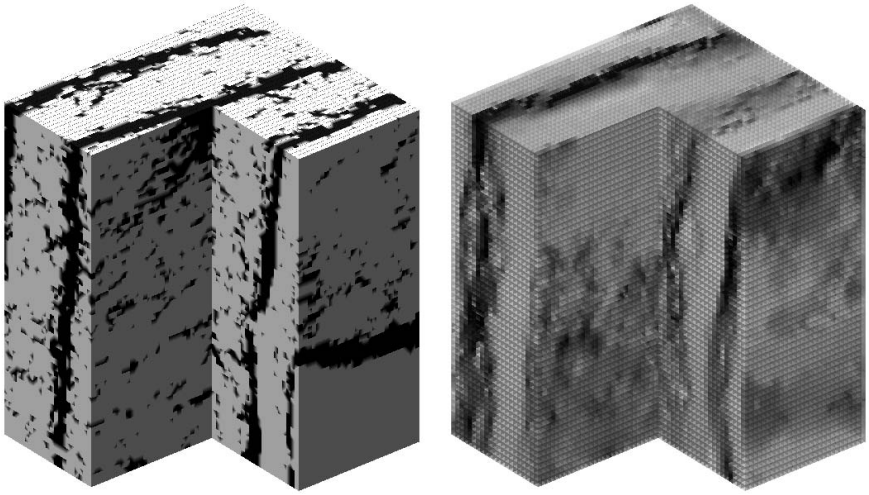

(a) Regions of elastin, in black. (b) Shear strain under torsion

Fig. 5. Large-scale simulation to study the mechanical response of a of 50^3 μm^3 sample of blood-vessel microstructure. The material distribution in the mesh is shown on the left, with black for elastin and gray for everything else. Contour plots of the shear strain are depicted on the right. Each solution took approximately one hour in 512 processors, enabling the study of multiple loading conditions in a single day

We describe next the construction of $D_{\mathrm{DG}}u_h$ in the simplest case, when $u_h = 0$ on $\partial\Omega$, where Ω is the domain, and the same discrete space V_h contains u_h and each component of $D_{\mathrm{DG}}u_h$. The more general case can be found in [9]. The starting point is the following integration by parts identity:

$$\sum_{E\in\mathcal{T}_h}\int_E \nabla u_h\cdot w\,dV = \int_{\Gamma_I}\left(\llbracket u_h\rrbracket\cdot\{w\}+\{u_h\}\cdot\llbracket w\rrbracket\right)\,dS - \sum_{E\in\mathcal{T}_h}\int_E u_h\nabla\cdot w\,dV, \tag{1}$$

valid for any $w\in V_h^d$, where d is the number of components of ∇u_h. Here Γ_I indicates the set of all element faces in the mesh that do not lie on $\partial\Omega$. The jump $\llbracket\cdot\rrbracket$ and average $\{\cdot\}$ operators are defined as

$$\llbracket v\rrbracket = v^+n^+ + v^-n^- \qquad \{v\} = \frac{1}{2}(v^+ + v^-), \tag{2}$$

where $v^\pm$ denotes the trace of v on either side of a face, and $n^\pm$ the corresponding external unit normal. An eminently intuitive idea for the definition of $D_{\mathrm{DG}}u_h$ consists in assuming that u is well approximated by u_h in the interior of every element, and by $\{u_h\}$ at element boundaries. An approximation of ∇u can then be constructed by requesting $D_{\mathrm{DG}}u_h$ to satisfy an equation similar to (1), namely

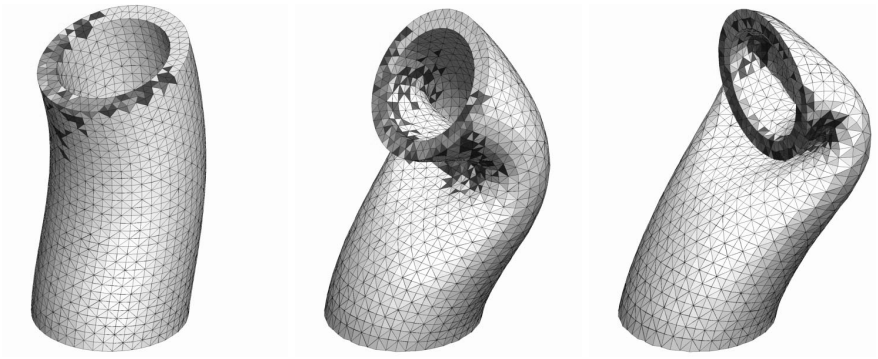

Fig. 6. Snapshots along the loading path of a nonlinear elastic cylinder. An adaptive stabilization strategy was adopted here, to automatically adjust the energetic cost of discontinuities as the deformation evolves. A nonzero stabilization term has been added only in the set of colored elements: the darker the color, the stiffer the term.

$$\sum_{E\in\mathcal{T}_h}\int_E D_{\mathrm{DG}}u_h\cdot w\,dV=\int_{\Gamma_I}\{u_h\}\cdot[\![w]\!]\,dS-\sum_{E\in\mathcal{T}_h}\int_E u_h\nabla\cdot w\,dV, \tag{3}$$

for any $w\in V_h^d$, where we have taken advantage that $[\![\{u_h\}]\!]=0$. Alternative DG methods are obtained by assuming other approximations of u at element boundaries. Fortunately, it is possible to explicitly solve (1) and (3) for $D_{\mathrm{DG}}u_h$ as a function of u_h to obtain

$$D_{\mathrm{DG}}u_h=\nabla u_h+R([\![u_h]\!]) \tag{4}$$

in the interior of every element E. Here R is a linear operator on $[\![u]\!]$ that returns a function in V_h^d, and that can be precomputed for any given mesh, see [1, 9]. Notice that when u_h is continuous, (4) simply returns the standard definition of a derivative. Finally, when non-homogeneous Dirichlet boundary conditions are present, they can either be incorporated into $D_{\mathrm{DG}}u_h$ for weak enforcement, or simply constrain V_h to satisfy them.

4 Application: Nonlinear Elasticity

The nonlinear elasticity problem consists in finding local minimizers of the potential energy functional within some suitable functional space V^d. Its DG approximation is obtained by simply finding a local minimizer φ_h in V_h^d of the discrete potential energy functional

$$I_h[\varphi_h]=\sum_{E\in\mathcal{T}_h}\int_E\left[W(D_{\mathrm{DG}}\varphi_h)-f\cdot\varphi_h\right]\,dV. \tag{5}$$

Here W is the strain energy density and f the body force per unit volume. The examples in Figs. 1, 2, 4 and 5 have all been obtained in this way.

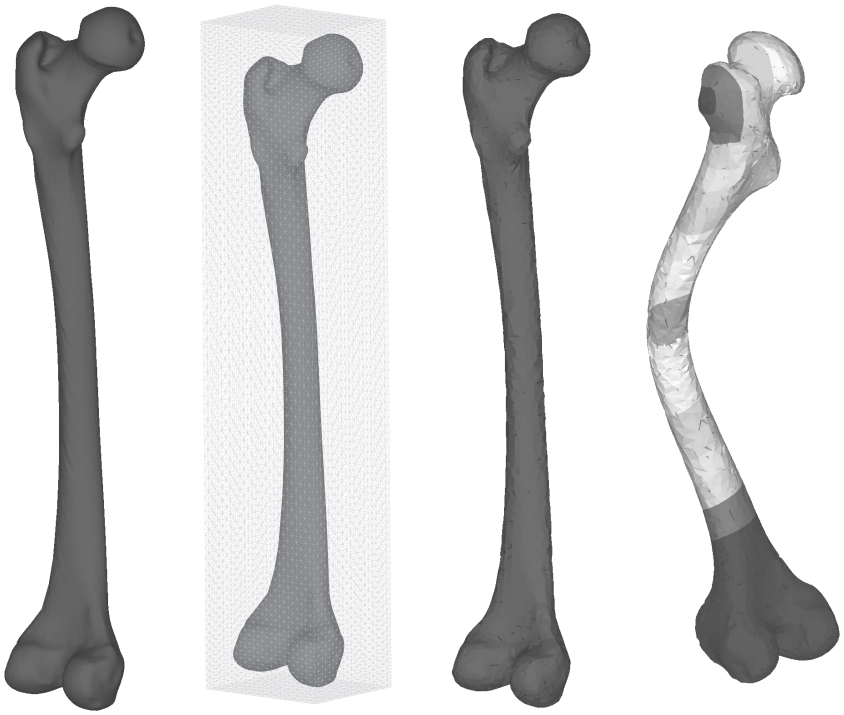

(a) Original (b) Immersed (c) Approximate (d) Deformed

Fig. 7. Three-dimensional example of a femur simulated with a DG-based immersed boundary method. The original geometry in Fig. 7(a) is immersed in a mesh of tetrahedra, Fig. 7(b). An approximate geometry is extracted, shown in Fig. 7(c), which is then subjected to compressive loads on its two ends. Modeled as a linear elastic material, the amplitude of deformations in Fig. 7(d) have been amplified for clarity. The DG-IBM method sidesteps the creation of meshes in complicated geometry while retaining an optimal order of convergence

A crucial difficulty encountered when relaxing the continuity constraint across element boundaries is that often $V_h^d \not\subseteq V^d$. One of its consequences is that the potential energy I_h is not guaranteed to even have a finite lower bound in V_h^d, and often it does not. The standard strategy in this case is to add a stabilization term to (5), in the form of a potential energy cost for each discontinuity in the solution, see [16, 17]. When the energetic cost of jumps is large enough, a *stable* scheme is recovered.

A delicate balance is required then. The additional term should be large enough to stabilize the problem, but not too large to essentially prevent any discontinuity from appearing. For classical linear elasticity the "right" size of the stabilization term is known [13], but in general its fully automatic and efficient selection is still an open problem. We have recently made some

progress by introducing the idea of adaptive stabilization [16, 17], but more comprehensive solutions may still be possible, see Fig. 6.

Finally, the convergence of the method for the classical linear elasticity problem was proved in [13]. Since each approximate solution as the mesh is refined is not even in H^1, the convergence of displacements was proved in the space of functions of bounded variations to any exact solution in H^2. Furthermore, displacements and stresses converge in L^2. In the nonlinear elastic case the convergence for the simpler case of a convex strain energy density was obtained in [3], by Gamma-convergence.

5 Application: A DG-based immersed boundary method

The two key ingredients in the construction of an immersed boundary method (IBM) are the approximation of the domain and how boundary conditions are imposed. Both need to work cooperatively to retain an optimal order of convergence. This is the reason for the profusion of first order methods, the crafting of complicated schemes to recover second-order, and the nearly absolute absence of high-order ones. These and other aspects in the case of homogeneous Dirichlet boundary conditions on $\partial\Omega$ are extensively discussed in [12], while the non-homogeneous case is the subject of an upcoming manuscript. A three-dimensional application of the DG-based IBM to elasticity is shown in Fig. 7, obtained by simply introducing discontinuities across the boundaries of all elements intersected by the immersed boundary, and finding the stationary points of (5).

References

1. D. N. Arnold, F. Brezzi, B. Cockburn, and L. D. Marini. Unified analysis of discontinuous Galerkin methods for elliptic problems. *SIAM J. Numer. Anal.*, 39:1749–1779, 2002.
2. D.N. Arnold, F. Brezzi, and L.D. Marini. A Family of Discontinuous Galerkin Finite Elements for the Reissner–Mindlin Plate. *Journal of Scientific Computing*, 22(1):25–45, 2005.
3. A. Buffa and C. Ortner. Variational convergece of IP–DGFEM. Technical Report 07/10, Oxford University Computing Laboratory, Numerical Analysis Group, Wolfson Building, Parks Road, Oxford, England OX1 3QD, April 2007.
4. F. Celiker, B. Cockburn, and H.K. Stolarski. Locking-Free Optimal Discontinuous Galerkin Methods for Timoshenko Beams. *SIAM Journal on Numerical Analysis*, 44:2297, 2006.
5. B. Cockburn and C.W. Shu. Runge-Kutta discontinuous Galerkin methods for convection-dominated problems. *J. Sci. Comput*, 16(3):173–261, 2001.
6. J.K. Djoko, F. Ebobisse, A.T. McBride, and B.D. Reddy. A discontinuous Galerkin formulation for classical and gradient plasticity–Part 1: Formulation and analysis. *Computer Methods in Applied Mechanics and Engineering*, 196(37-40):3881–3897, 2007.

7. J.K. Djoko, F. Ebobisse, A.T. McBride, and B.D. Reddy. A discontinuous Galerkin formulation for classical and gradient plasticity. Part 2: Algorithms and numerical analysis. *Computer Methods in Applied Mechanics and Engineering*, 197(1-4):1–21, 2007.
8. G. Engel, K. Garikipati, T.J.R. Hughes, M.G. Larson, L. Mazzei, and R.L. Taylor. Continuous/discontinuous finite element approximations of fourth-order elliptic problems in structural and continuum mechanics with applications to thin beams and plates, strain gradient elasticity. *Computer Methods in Applied Mechanics and Engineering*, 191:3669–3750, 2002.
9. A. Ten Eyck and A. Lew. Discontinuous Galerkin methods for nonlinear elasticity. *Internat. J. Numer. Methods Engrg.*, 67:1204–1243, 2006.
10. S. Guzey, B. Cockburn, and HK Stolarski. The embedded discontinuous Galerkin method: Application to linear shell problems. *Int. J. Numer. Meth. Engng*, 70:757–790, 2007.
11. P. Hansbo and MG Larson. Discontinuous Galerkin methods for incompressible and nearly incompressible elasticity by Nitsche's method. *Computer Methods in Applied Mechanics and Engineering*, 191(17):1895–1908, 2002.
12. A. Lew and G. Buscaglia. A discontinuous-Galerkin-based immersed boundary method. *International Journal for Numerical Methods in Engineering*, 2008. in press.
13. A. Lew, P. Neff, D. Sulsky, and M. Ortiz. Optimal BV estimates for a discontinuous Galerkin method in linear elasticity. *Applied Mathematics Research Express*, 3:73–106, 2004.
14. L. Noels and R. Radovitzky. A new discontinuous Galerkin method for Kirchhoff-Love shells. http://asap.mit.edu/publications/journal/cmame-2007.pdf, 2007.
15. M. O'Connel and C. Taylor. Personal communication, 2007. Stanford University.
16. A. Ten Eyck, F. Celiker, and A. Lew. Adaptive stabilization of discontinuous Galerkin methods for nonlinear elasticity: Analytical estimates. *Computer Methods In Applied Mechanics and Engineering*, 2008. In press.
17. A. Ten Eyck, F. Celiker, and A. Lew. Adaptive stabilization of discontinuous Galerkin methods for nonlinear elasticity: Motivation, formulation and numerical examples. *Computer Methods In Applied Mechanics and Engineering*, 2008. In press.
18. G.N. Wells and N.T. Dung. A C0 discontinuous Galerkin formulation for Kirchhoff plates. *Computer Methods in Applied Mechanics and Engineering*, 196(35-36):3370–3380, 2007.
19. G.N. Wells, E. Kuhl, and K. Garikipati. A discontinuous Galerkin method for the Cahn–Hilliard equation. *Journal of Computational Physics*, 218(2):860–877, 2006.
20. T.P. Wihler. Locking–free DGFEM for elasticity problems in polygons. *IMA Journal of Numerical Analysis*, 24:45–75, 2004.